Chance-constrained Real-time Pricing of Reserves Incorporating System Frequency Dynamics

Bo Chen, *Student Member, IEEE*, and Yu Christine Chen, *Member, IEEE*

***Abstract*—This paper presents a method to internalize the impact of system frequency dynamics into real-time pricing of reserves. The proposed frequency dynamics-aware price of reserves helps to incentivize and compensate generators for setting aside reserves that contribute to de-risking real-time dynamic performance subject to uncertainty in the net-load forecast. Central to the proposed method is to augment a static chance-constrained economic dispatch (CCED) with constraints modelling system frequency dynamics driven by generator inertia response along with primary and secondary frequency controls. Chance constraints in the resulting dynamics-aware CCED enforce tolerable probability of dynamic system frequency and generator power trajectories violating their respective limits. We show that the dynamics-aware price of reserves internalizes uncertainty in dynamic state variables along with the risk of violating limits in frequency excursions and generator outputs during frequency transients as well as at steady state. We also assess the sensitivity of the dynamics-aware price of reserves with respect to generator parameters that directly affect system dynamic performance. Numerical case studies involving the Western System Coordinating Council and New England test systems confirm dynamics in the proposed price of reserves, reveal additional revenue for generators, and demonstrate computational scalability.**

***Index Terms*—Chance constraints, economic dispatch, frequency dynamics, pricing of reserves, uncertainty**

I. Introduction

Extensive integration of renewable energy sources (RESs) helps to address burgeoning environmental concerns associated with fossil fuel-based generators. However, deploying low-inertia RESs in the power system leads to larger, faster, and more frequent variations in its net load—load minus non-dispatchable RES generation—thereby presenting notable challenges for reliable and efficient operation [1]. Real-time supply-demand balancing is made even more difficult by considerable uncertainty in forecasting RES generation, which in turn calls for ever more operating reserves [2]. However, additional reserves procured via new construction of fast-response generators, e.g., combustion turbines, can cause more emissions. A promising alternative involves having (possibly a subset of) inverter-based RESs and battery storage devices contribute to balancing the net demand *and* providing sufficient reserves to offset forecast uncertainty, both on a second-to-second basis, alongside existing turbine-based generators. While technically feasible with modern power-electronic inverters furnished with frequency-responsive controllers, crucial for real-world uptake of this potential solution are market structures that seamlessly integrate services provided by inverter- and turbine-based assets and offer suitable compensation for supplying energy and contributing to reserves to support real-time dynamic and steady-state performance [3].

Central to the real-time electricity market problem is an economic dispatch (ED) traditionally solved assuming that the net-load forecast is known precisely [4]. For example, both the Alberta Electric System Operator and PJM solve a real-time ED every five minutes to minimize dispatch cost in a co-optimization of energy and reserves to respectively serve a deterministic load forecast and satisfy an explicit reserve requirement for the system [5], [6]. Extensive integration of RESs has motivated stochastic market designs that embed probabilistic models of the growing uncertainty in the net-load forecast. These facilitate the procurement of sufficient reserves alongside the optimal dispatch of energy, thereby ensuring that adequate capacity is available to handle potentially large fluctuations in the net load across the scheduling horizon [7]. Accompanying the optimal market-clearing solutions are prices that then inform payments to be made to generators for the energy that they produce and the reserves that they set aside. The price of energy generally captures the marginal cost of optimally supplying an additional unit of electric load considering the cost of generation constrained by supply-demand balance and generator capacity limits [8], and the price of reserves covers the opportunity cost for a generator to maintain available capacity on standby [9].

Prior work in stochastic markets includes scenario-based optimization [10], robust optimization [11], and chance-constrained optimization [12]. These generally modify a deterministic ED (or ED-like) problem with costs and constraints that enable uncertainty-aware decision-making and pricing consistent with a particular choice of model for the net-load forecast uncertainty. For example, [12] minimizes the expected cost of generation while enforcing tolerable probability of constraint violations given moment-based net-load forecast probabilistic models, leading to the formulation of a chance-constrained economic dispatch (CCED). The CCED avoids trading off between expected and per-scenario performance typical in scenario-based methods and potentially overly conservative decisions from robust optimization [12]. However, in general, the aforementioned prior efforts in stochastic markets do not capture the cost of setting aside sufficient reserves to handle transient frequency excursions expected to become larger and more frequent in future power systems due to the displacement of high-inertia turbine-based generators with low-inertia inverter-based resources. In this paper, we extend a static CCED into a multi-interval multi-time scale optimization problem and derive the ensuing real-time *dynamics-aware* price of reserves and compensation for generators. The result-

Authors are affiliated with the Department of Electrical and Computer Engineering at The University of British Columbia, Vancouver, Canada. E-mail: {cbhp1993, chen}@ece.ubc.ca. They gratefully acknowledge the support of the Natural Sciences and Engineering Research Council of Canada (NSERC), funding reference number RGPIN-2023-05240.

ing price represents the marginal cost of setting aside reserve capacity, for an incremental change in net-load uncertainty, to limit the risk of violating frequency and power generation constraints during system frequency transients as well as at steady state.

Although the dynamics-aware price of reserves derives from the optimal solution of an ED (or a CCED more precisely), the focus of this paper is not on frequency-constrained dispatch of conventional and inverter-based resources toward favourable dynamic frequency response (see, e.g., [13]–[15] and references therein). Instead, our aim is to compensate generators for de-risking system dynamic performance under uncertainty and pricing thereof, which has motivated recent work in procuring *new* services, such as physical or virtual inertia [16]–[20], fast frequency response reserves [17]–[19], and primary frequency response reserves [17]–[20], to mitigate undesirable frequency excursions. However, the proposition of creating new products may be challenged by potential downstream effects on generators' strategic participation in existing markets and opportunity costs incurred by having more market products. Thus, we seek to extend *existing* real-time markets in, e.g., [5], [6], that co-optimize energy and reserves *without* creating any new products or services. Instead, the extension lies in pricing reserves set aside by generators toward restoring frequency to synchronous steady state and de-risking dynamic performance in the face of uncertainty in net load. With respect to dynamic modelling, prior literature tends to formulate common dynamic performance requirements on, e.g., rate of change of frequency [16]–[20], magnitude of frequency deviation [17]–[20], and primary frequency response [18]–[20], as *algebraic* approximations and incorporate them as constraints in an economic dispatch. Unlike these algebraic approximations valid only at specific snapshots in time, in this paper, we directly incorporate frequency dynamics that capture the time-domain dynamic response in its entirety across the scheduling horizon. We have made use of this general approach in [21]–[23] to derive dynamics-aware price of energy. Specifically, [21]–[23] modify a static ED to formulate multi-interval multi-time scale *dynamics-aware* EDs that embed constraints modelling relatively fast frequency dynamics ascribed to (potentially virtual) synchronous generators and slower set-point decisions from secondary frequency control.

This paper extends the deterministic EDs in [21], [22] subject to precise forecasts of net load by modelling probabilistic uncertainty therein and formulating a dynamics-aware CCED where chance constraints enforce tolerable probability of dynamic system frequency and generator power trajectories violating their respective limits. Furthermore, unlike the dynamics-aware CCED in [23] that penalizes the expected value of system frequency deviations in the objective function to enable secondary frequency control, the problem in this paper is formulated to reflect actual system operations by incorporating a dynamical model of an industry-standard automatic generation control (AGC). With uncertainty in the net-load forecast across the scheduling horizon modelled as a Gaussian random variable, the dynamics-aware CCED reformulates into a deterministic optimization problem with quadratic cost and linear constraints that can be solved at scale using off-the-shelf optimization packages. From the optimal solution, we derive the real-time price of *reserves* as the marginal cost incurred to optimally offset an incremental change in the net-load uncertainty while satisfying dynamic chance constraints. We demonstrate that, unlike the uncertainty-oblivious price of energy studied in [21]–[23], the dynamics-aware price of reserves internalizes uncertainty in dynamic decision variables as well as the risk of violating limits in frequency excursions and generator outputs across system transients and into steady state. Finally, extensive numerical simulations involving the Western System Coordinating Council (WSCC) 3-generator and New England 10-generator test systems confirm dynamics in the proposed price of reserves, underscore its dependence on generator parameters that directly affect system dynamic risk profile, reveal additional revenue for generators, and demonstrate computational scalability.

The remainder of the paper is organized as follows. Section II outlines the static CCED and pertinent dynamical models for the AGC and generators. In Section III, we formulate the dynamics-aware CCED and model probabilistic uncertainty in its decision variables. Section IV presents main results on the proposed dynamics-aware price of reserves. Section V provides extensive numerical simulations involving two standard test systems. Finally, we offer concluding remarks and directions for future work in Section VI.

II. Preliminaries

This section presents a static CCED incorporating net-load forecast uncertainty for a stochastic market followed by models of the AGC and generators pertinent to system dynamic frequency response. Then, via a numerical example, we motivate the need to embed dynamics into pricing of reserves.

A. Static Chance-constrained Economic Dispatch

Consider a transmission system with G online generators in the set $\mathcal{G} = \{1, \ldots, G\}$ supplying forecasted net load (inclusive of must-take renewable generation and losses) $P_\circ^{\text{load}}$. Prevailing static ED formulations assume that the power system operates at synchronous steady state. Suppose generator g produces steady-state electrical power $P_{g,\circ}$ with cost function $C_g(P_{g,\circ})$. Given $P_{g,\circ}$ subject to uncertainty due to imprecise predictions of the upcoming load demand and renewable generation, the total expected cost of generation is $\mathbb{E}[C(P_\circ)] = \mathbb{E}[\sum_{g\in\mathcal{G}} C_g(P_{g,\circ})]$, where $P_\circ = [P_{1,\circ}, \ldots, P_{G,\circ}]^{\mathrm{T}}$. A static single-snapshot CCED can be formulated as (see, e.g., [12])

$$\begin{aligned}
\underset{P_\circ,\pi}{\text{minimize}} \quad & \mathbb{E}[C(P_\circ)] && \text{(1a)}\\
\text{subject to} \quad & \mathbb{1}_G^{\mathrm{T}} P_\circ = P_\circ^{\text{load}}, && \text{(1b)}\\
& P_\circ = \pi P_\circ^{\text{load}}, && \text{(1c)}\\
& \mathbb{P}(P_\circ \geq P_{\min}) \geq (1-\varepsilon^P)\mathbb{1}_G, && \text{(1d)}\\
& \mathbb{P}(P_\circ \leq P_{\max}) \geq (1-\varepsilon^P)\mathbb{1}_G, && \text{(1e)}
\end{aligned}$$

where participation factors collected in $\pi \in \mathbb{R}^G$ distribute system net load and uncertainty therein amongst all generators, $\varepsilon^P \in (0,1)$ represents the tolerable probability of violating chance constraints in (1d)–(1e), and $\mathbb{1}_G$ is a G-dimensional

vector of 1s. The scalar variable $P_\circ^{\text{load}}$ can be modelled using statistical moments of the underlying uncertainty via a Gaussian distribution, in which case $P_\circ$ would follow a joint Gaussian distribution in accordance with (1c). The CCED in (1) can then be reformulated into a convex deterministic optimization problem that can be solved efficiently at scale [12].

B. System Frequency Dynamics

Let $P^{\text{r}} = [P_1^{\text{r}}, \dots, P_G^{\text{r}}]^{\text{T}}$, where P_g^{r} denotes the reference set-point of generator $g \in \mathcal{G}$. For a single-area power system, P^{r} is obtained as [24]

$$P^{\text{r}} = P_\circ + \pi(\xi - \mathbb{1}_G^{\text{T}} P_\circ), \tag{2}$$

where $P_\circ$ represents the most recent optimal solution of a static ED and accompanying a linear perturbative analysis thereof around that optimal solution are AGC participation factors collected in $\pi = [\pi_1, \dots, \pi_G]^{\text{T}}$, with $\pi_g \geq 0$, $\forall\, g \in \mathcal{G}$ and $\mathbb{1}_G^{\text{T}} \pi = 1$. Furthermore, in (2), ξ is the AGC state variable with dynamics modelled by [24]

$$\tau_{\text{A}} \dot{\xi} = -\xi - \text{ACE} + P^{\text{load}}, \tag{3}$$

where τ_{A} is the AGC time constant typically ranging from 30 [sec] to minutes [25], $\text{ACE} = -k\beta\Delta\omega$ is the area control error (ACE) for a single-area power system, and the system load P^{load} must be balanced by electrical outputs summed across all generators at any given time. The ACE is calculated by scaling $\Delta\omega = \omega - \omega_{\text{s}}$, where ω denotes the prevailing frequency for the area and $\omega_{\text{s}} = 2\pi 60\,[\text{rad/s}]$ is the synchronous speed, by the product of a constant $k < 0$ and the area's bias factor β. The value of the bias factor is typically set as the area's frequency-response characteristic [24], [26]. The model in (2)–(3) is equivalent to the control block diagram depicted in [24, p. 494], and it can easily extend to the case of multiple areas (see, e.g., [27]) at the expense of greater notational burden. Regarding time-scales of operation, industry implementations of the AGC generally sample the ACE signal and then update the generator reference set-points every two to four seconds [25], [26]. These serve to inform the longer time step in the dynamics-aware CCED to be formulated in Section III, where we extract values for $\Delta\omega$ for the ACE signal via dynamical models outlined next.

Let $P^{\text{m}} = [P_1^{\text{m}}, \dots, P_G^{\text{m}}]^{\text{T}}$, where P_g^{m} denotes the turbine mechanical power of generator $g \in \mathcal{G}$. Assuming that electrical distances amongst different generators in the system are negligible, the electrical angular frequency of generator $g \in \mathcal{G}$, denoted by ω_g, would follow the same transient behaviour as all other generators with $\omega_g = \omega$, $\forall\, g \in \mathcal{G}$ [28]. Then dynamics in the system frequency deviations $\Delta\omega := \omega - \omega_{\text{s}}$ for the time-scales of our interest can be modelled by

$$M_{\text{eff}} \Delta\dot{\omega} = \mathbb{1}_G^{\text{T}} P^{\text{m}} - D_{\text{eff}} \Delta\omega - P^{\text{load}}, \tag{4}$$

$$\tau \dot{P}^{\text{m}} = P^{\text{r}} - P^{\text{m}} - R^{-1} \mathbb{1}_G \Delta\omega, \tag{5}$$

where $M_{\text{eff}} := \sum_{g\in\mathcal{G}} M_g$ with M_g denoting the inertia constant of generator g, $D_{\text{eff}} := \sum_{g\in\mathcal{G}} D_g$ with D_g denoting the damping constant of generator g, and $\tau = \text{diag}([\tau_1, \dots, \tau_G]^{\text{T}})$ and $R^{-1} = \text{diag}([R_1^{-1}, \dots, R_G^{-1}]^{\text{T}})$ respectively collect the turbine-governor time constants and inverse-droop constants of all generators [26]. The model in (4)–(5) is of order $G+1$, where each entry in (5) is constructed for an individual generator (or aggregate power plant), so the model indeed distinguishes amongst response speeds and droop characteristics of different generators. Moreover, dynamic frequency support from inverter-based resources can be readily incorporated into (4)–(5) by controlling the active-power loops as so-called *virtual synchronous generators* [29]. Finally, the system initially operates at steady-state equilibrium with $\omega(0) = \omega_{\text{s}}$ given the initial net load $P^{\text{load}}(0) = P_\circ^{\text{load}} = \sum_{g\in\mathcal{G}} P_{g,\circ}^{\text{r}}$, with generator g initially operating at $P_g^{\text{r}}(0) = P_g^{\text{m}}(0) = P_{g,\circ}^{\text{r}}$.

TABLE I: Dynamic parameter values for generators in the WSCC test system (boldface distinguishes values that *differ* from the default in the standard test case).

Generator	Case(s)	M_g [sec]	D_g	R_g^{-1}	τ_g [sec]
$g = 1$	1, 2, 3	23.64	20	100	2
$g = 2$	1, 2, 3	6.4	20	100	2
$g = 3$	1	3.01	20	**0**	2
	2	3.01	20	100	2
	3	**13.01**	**50**	**125**	**1**

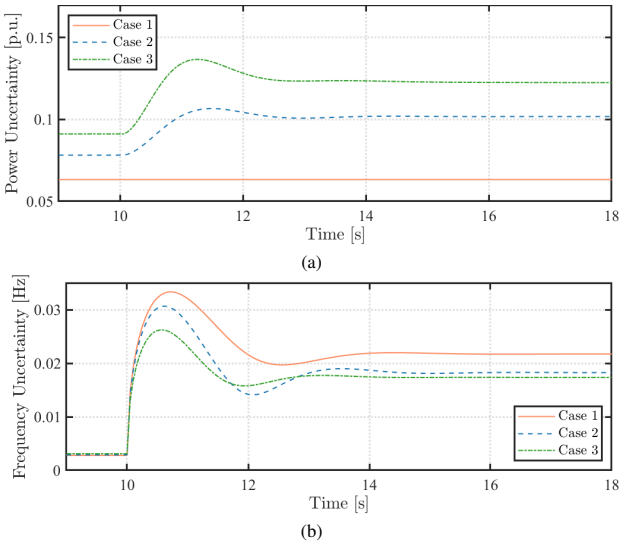

Fig. 1: (Example 1). Dynamic trajectories in uncertainty realized by setting generator parameters to values provided in Table I in response to an increase in net load associated with Gaussian uncertainty: standard deviation values of the marginal uncertainty distribution of (a) mechanical power of the most expensive generator and (b) system frequency deviations.

C. Problem Statement

The static CCED in (1) does not explicitly model system dynamics, so subsequent solutions lack insight into pricing during frequency transients. Consequently, approaches relying on static models to price reserves do not offer explicit incentives or compensation to generators for supporting system dynamic frequency response, as we demonstrate next.

Example 1 (WSCC 3-Generator Test System)**.** Consider the WSCC test system from [30] consisting of two cheaper generators and a more expensive third. We solve the static CCED in (1) with uncertainty in the net-load forecast modelled as a Gaussian random variable with zero mean and standard deviation 0.2 [p.u.]. We examine system dynamics in response to a 20% increase in the nominal (or mean) values of all

loads at time $t = 10\,[\text{sec}]$ under three sets of generator parameter values given in Table I, where generator 3 does not contribute to primary frequency response in case 1 with $R_3^{-1} = 0$, otherwise all parameters in cases 1 and 2 take their default values from the standard test system. In each case, we perform 1,000 independent dynamic simulations, each of which randomly samples Gaussian uncertainty in net load that then propagates to uncertainty in system dynamic states. From the resulting simulated trajectories of the mechanical power of the most expensive generator, i.e., generator 3, and the system frequency deviations, we calculate their standard deviation at each time step and plot them in Fig. 1.

In Fig. 1a, the uncertainty trajectory for generator 3 in case 1 remains constant during the simulation period and is thus consistent with the steady-state assumption under which the static CCED is solved. On the other hand, in Fig. 1b, case 2 depicted in blue colour ostensibly represents more desirable risk profile for the system with lower uncertainty in frequency deviations than case 1 in red colour. Case 3 further ascribes values for inertia, damping, droop, and turbine-governor time constants of generator 3 that exposes system frequency deviations to even lower uncertainty, as highlighted in green colour in Fig. 1b. Clearly, the uncertainty distributions for dynamic state variables vary over time and across the three cases. However, these differences are not captured by the static CCED in (1) because frequency dynamics are not modelled, and (1c) requires the net load (and its uncertainty) to distribute across generators in proportion to constant participation factors in π *regardless* of their contribution to support the system's dynamic risk profile over time. ■

The example above highlights that generators and system frequency deviations are, in fact, exposed to varying levels of uncertainty and thereby risk over time, contrary to the steady-state assumption implicit in static CCED. However, the price at which generators are conventionally compensated for putting aside reserve capacity is determined under the steady-state assumption. Also, parameter values of generators (and inverter-based resources) impact their dynamic response to disturbances and lead to varying levels of risk exposure. However, conventional frequency regulation services generally do not compensate generators explicitly for the risk that they undertake during transients based on their contribution to system dynamic performance, and only sometimes for response speed under additional so-called mileage payments. Finally, fast-response inverter-based resources that can participate in inertial or primary frequency response alongside conventional generators do not yet do so [19]. To address these issues, we generalize the static CCED in (1) and the resulting price of reserves to embed the effects of frequency dynamics, with the overarching goal being to provide conventional generators and inverter-based resources alike with compensation that is consistent with their contribution to supporting dynamic frequency performance under net-load forecast uncertainty.

III. Dynamics-aware CCED

This section formulates the dynamics-aware CCED by generalizing over the problem in (1). We then model uncertainty in the net load and system dynamic state variables and reformulate the CCED into a deterministic optimization problem.

A. Chance-constrained Problem Formulation

For the CCED problem, consider a scheduling horizon from time t_0 to $t_0 + T$ with, e.g., length $T = 5\,[\text{min}]$, for real-time markets. We subdivide the scheduling horizon according to longer time steps of length Δt^{S} (e.g., $5\,[\text{sec}]$) reflecting the granularity of slower AGC action to adjust generator reference set-points and shorter time steps of length Δt^{D} (e.g., $0.05\,[\text{sec}]$) adequately capturing faster generator frequency dynamics. The two time steps Δt^{S} and Δt^{D} respectively subdivide the scheduling horizon into equal intervals with endpoints collected in the sets $\mathcal{T}_{t_0}^{\text{S}} = \{t_0, t_0+\Delta t^{\text{S}}, \dots, t_0+T\}$ and $\mathcal{T}_{t_0}^{\text{D}} = \{t_0, t_0 + \Delta t^{\text{D}}, \dots, t_0 + T\}$.

The proposed dynamics-aware CCED incorporates one set of ED set-points across the entire scheduling horizon of length T, generator reference set-points determined by the AGC at intervals of Δt^{S}, and frequency dynamics updated at intervals of Δt^{D}. Due to forecast errors, the upcoming net load over the scheduling horizon P_t^{load}, $t \in \mathcal{T}_{t_0}^{\text{D}}$, is not known precisely and uncertainty is associated with decision variables. The dynamics-aware CCED is then formulated as follows:

$$\underset{\Omega}{\text{minimize}} \sum_{t\in\mathcal{T}_{t_0}^{\text{D}}} \mathbb{E}[C(P_t^{\text{m}})]\Delta t^{\text{D}} \tag{6a}$$

$$\text{subject to } M_{\text{eff}}\Big(\frac{\Delta\omega_{t+\Delta t^{\text{D}}} - \Delta\omega_t}{\Delta t^{\text{D}}}\Big) = \mathbb{1}_G^{\text{T}} P_t^{\text{m}} - D_{\text{eff}}\Delta\omega_t - P_t^{\text{load}},\ t \in \mathcal{T}_{t_0}^{\text{D}} \setminus \{t_0 + T\}, \tag{6b}$$

$$\tau\Big(\frac{P_{t+\Delta t^{\text{D}}}^{\text{m}} - P_t^{\text{m}}}{\Delta t^{\text{D}}}\Big) = P_{t'}^{\text{r}} - P_t^{\text{m}} - R^{-1}\mathbb{1}_G\Delta\omega_t,\ t' \in \mathcal{T}_{t_0}^{\text{S}} \setminus \{t_0 + T\},\ t \in \{t', \dots, t' + \Delta t^{\text{S}} - \Delta t^{\text{D}}\}, \tag{6c}$$

$$\tau_{\text{A}}\Big(\frac{\xi_{t'+\Delta t^{\text{S}}} - \xi_{t'}}{\Delta t^{\text{S}}}\Big) = -\xi_{t'} + k\beta\Delta\omega_{t'} + P_{t'}^{\text{load}},\ t' \in \mathcal{T}_{t_0}^{\text{S}} \setminus \{t_0 + T\}, \tag{6d}$$

$$P_{t'}^{\text{r}} = P_\circ + \pi(\xi_{t'} - \mathbb{1}_G^{\text{T}} P_\circ),\ t' \in \mathcal{T}_{t_0}^{\text{S}}, \tag{6e}$$

$$\mathbb{1}_G^{\text{T}} P_\circ = \frac{1}{|\mathcal{T}_{t_0}^{\text{D}}|} \sum_{t\in\mathcal{T}_{t_0}^{\text{D}}} P_t^{\text{load}}, \tag{6f}$$

$$\mathbb{P}(\Delta\omega_t \le \Delta\omega_{\max}) \ge 1 - \varepsilon^{\omega},\ t \in \mathcal{T}_{t_0}^{\text{D}}, \tag{6g}$$

$$\mathbb{P}(\Delta\omega_t \ge \Delta\omega_{\min}) \ge 1 - \varepsilon^{\omega},\ t \in \mathcal{T}_{t_0}^{\text{D}}, \tag{6h}$$

$$\mathbb{P}(P_t^{\text{m}} \le P_{\max}^{\text{m}}) \ge \mathbb{1}_G(1 - \varepsilon^{P}),\ t \in \mathcal{T}_{t_0}^{\text{D}}, \tag{6i}$$

$$\mathbb{P}(P_t^{\text{m}} \ge P_{\min}^{\text{m}}) \ge \mathbb{1}_G(1 - \varepsilon^{P}),\ t \in \mathcal{T}_{t_0}^{\text{D}}, \tag{6j}$$

where $\Omega = \{P_\circ, P_{t'}^{\text{r}}, \xi_{t'}, P_t^{\text{m}}, \Delta\omega_t\}_{t\in\mathcal{T}_{t_0}^{\text{D}},\, t'\in\mathcal{T}_{t_0}^{\text{S}}}$ collects the decision variables of the optimization problem and $|\cdot|$ denotes the cardinality operator. The objective in (6a) is the expected value of operation cost $\mathbb{E}[C(P_t^{\text{m}})] = \mathbb{E}[\sum_{g\in\mathcal{G}} C_g(P_{g,t}^{\text{m}})]$ under uncertainty in net-load forecast. Amongst the constraints, discrete-time system dynamics in (6b)–(6e) result from a first-order approximation of the continuous-time dynamics in (2)–(5), where the generator and AGC dynamics are respectively discretized at shorter time steps of Δt^{D} and longer time steps of Δt^{S}. The value of Δt^{D} can be informed by a trade-off

between discretization accuracy and computational burden to solve (6), and the value of Δt^{S} reflects the AGC actuation interval. Instead of resorting to first-order approximation, (6b)–(6d) can readily be replaced by discrete-time dynamics synthesized from other discretization methods. Further, the constraint in (6f) enforces ED set-points across all generators to sum up to the net-load forecast averaged over the course of the scheduling horizon. Finally, chance constraints in (6g)–(6h) and (6i)–(6j) respectively impose ε^{ω} and ε^{P} as the tolerable probability of violating limits in system frequency and generator mechanical powers to, e.g., satisfy certain reliability criteria in a given system.

Remark 1 (Network Power Flow Constraints)**.** In (6), the inclusion of chance constraints on transmission line flows would be *methodologically* straightforward using injection shift factors, in a manner similar to the approach in [22]. However, this hypothetical approach would yield *locational* prices of reserves varying across the system instead of a single uniform price, unlike industry practice [5], [6], academic literature [10], [12], and standard textbook reasoning presented in, e.g., [4, Chap. 5.4], that advocate for pricing reserves centrally across a control area (or so-called "reserve zone" in the context of reserve procurement) to mitigate uncertainty in aggregate load (or other unpredictable events). In light of this, we deliberately impose power balance across the system in (6f) instead of at each individual bus. Moreover, the exclusion of network power flow equations is consistent with our intention to generalize over the static CCED in (1) imposing only system net power balance in (1b). ■

B. Uncertainty Models

We decompose the net-load forecast as

$$P_t^{\mathrm{load}} = \overline{P}_t^{\mathrm{load}} + \widetilde{P}_t^{\mathrm{load}},\ t \in \mathcal{T}_{t_0}^{\mathrm{D}}, \tag{7}$$

where $\overline{P}_t^{\mathrm{load}}$ is the nominal (or mean) value and $\widetilde{P}_t^{\mathrm{load}}$ represents the uncertain component. Following this, system dynamic state variables $\Delta\omega_t$, P_t^{m}, $\xi_{t'}$, and $P_{t'}^{\mathrm{r}}$ can each be similarly decomposed into two components, as follows:

$$\Delta\omega_t = \Delta\overline{\omega}_t + \Delta\widetilde{\omega}_t,\ t \in \mathcal{T}_{t_0}^{\mathrm{D}}, \tag{8}$$
$$P_t^{\mathrm{m}} = \overline{P}_t^{\mathrm{m}} + \widetilde{P}_t^{\mathrm{m}},\ t \in \mathcal{T}_{t_0}^{\mathrm{D}}, \tag{9}$$
$$\xi_{t'} = \overline{\xi}_{t'} + \widetilde{\xi}_{t'},\ t' \in \mathcal{T}_{t_0}^{\mathrm{S}}, \tag{10}$$
$$P_{t'}^{\mathrm{r}} = \overline{P}_{t'}^{\mathrm{r}} + \widetilde{P}_{t'}^{\mathrm{r}},\ t' \in \mathcal{T}_{t_0}^{\mathrm{S}}, \tag{11}$$

where $\overline{\cdot}$ denotes the nominal value of the corresponding state variable and $\widetilde{\cdot}$ denotes the component encapsulating its uncertainty. Substitution of (7)–(11) into (6b)–(6d) reveals that (6b)–(6d) can be equivalently expressed as the sum of two constituent linear dynamical systems. The first system in this sum models the mean trajectories of the dynamic state variables, as follows:

$$\begin{bmatrix}\Delta\overline{\omega}_{t+\Delta t^{\mathrm{D}}}\\ \overline{P}^{\mathrm{m}}_{t+\Delta t^{\mathrm{D}}}\end{bmatrix} = A\begin{bmatrix}\Delta\overline{\omega}_t\\ \overline{P}^{\mathrm{m}}_t\end{bmatrix} + B\overline{P}_t^{\mathrm{load}} + C\overline{P}^{\mathrm{r}}_{t'},$$
$$t' \in \mathcal{T}_{t_0}^{\mathrm{S}} \setminus \{t_0+T\},\ t \in \{t', \ldots, t'+\Delta t^{\mathrm{S}} - \Delta t^{\mathrm{D}}\}, \tag{12}$$
$$\overline{\xi}_{t'+\Delta t^{\mathrm{S}}} = a\overline{\xi}_{t'} + b\overline{P}_{t'}^{\mathrm{load}} + c\Delta\overline{\omega}_{t'},\ t' \in \mathcal{T}_{t_0}^{\mathrm{S}} \setminus \{t_0+T\}, \tag{13}$$

where matrices A, B, and C as well as scalar constants a, b, and c are given by

$$A = \begin{bmatrix} 1 - \frac{D_{\mathrm{eff}}}{M_{\mathrm{eff}}}\Delta t^{\mathrm{D}} & \frac{1}{M_{\mathrm{eff}}}\mathbb{1}_G^{\mathrm{T}}\Delta t^{\mathrm{D}} \\ -\tau^{-1}R^{-1}\mathbb{1}_G\Delta t^{\mathrm{D}} & \mathrm{diag}(\mathbb{1}_G) - \tau^{-1}\Delta t^{\mathrm{D}}\end{bmatrix},$$
$$B = \begin{bmatrix} -\frac{1}{M_{\mathrm{eff}}}\Delta t^{\mathrm{D}} \\ \mathbb{0}_G\end{bmatrix},\ C = \begin{bmatrix}\mathbb{0}_G^{\mathrm{T}} \\ \tau^{-1}\Delta t^{\mathrm{D}}\end{bmatrix},$$
$$a = 1 - \tau_{\mathrm{A}}^{-1}\Delta t^{\mathrm{S}},\ b = \tau_{\mathrm{A}}^{-1}\Delta t^{\mathrm{S}},\ c = \tau_{\mathrm{A}}^{-1}k\beta\Delta t^{\mathrm{S}}. \tag{14}$$

The second dynamical system in the sum models the uncertain components of the dynamic state variables, given by

$$\begin{bmatrix}\Delta\widetilde{\omega}_{t+\Delta t^{\mathrm{D}}}\\ \widetilde{P}^{\mathrm{m}}_{t+\Delta t^{\mathrm{D}}}\end{bmatrix} = A\begin{bmatrix}\Delta\widetilde{\omega}_t\\ \widetilde{P}^{\mathrm{m}}_t\end{bmatrix} + B\widetilde{P}_t^{\mathrm{load}} + \mathcal{O}_t C\widetilde{P}^{\mathrm{r}}_{t'},$$
$$t' \in \mathcal{T}_{t_0}^{\mathrm{S}} \setminus \{t_0+T\},\ t \in \{t', \ldots, t'+\Delta t^{\mathrm{S}} - \Delta t^{\mathrm{D}}\}, \tag{15}$$
$$\widetilde{\xi}_{t'+\Delta t^{\mathrm{S}}} = a\widetilde{\xi}_{t'} + b\widetilde{P}_{t'}^{\mathrm{load}} + c\Delta\widetilde{\omega}_{t'},\ t' \in \mathcal{T}_{t_0}^{\mathrm{S}} \setminus \{t_0+T\}, \tag{16}$$

where the indicator variable $\mathcal{O}_t = 1$ if $t \in \mathcal{T}_{t_0}^{\mathrm{S}}$ and $\mathcal{O}_t = 0$ otherwise. The same decomposition further enables (6e) to be expressed as the sum of the following two components:

$$\overline{P}_{t'}^{\mathrm{r}} = P_{\circ} + \pi(\overline{\xi}_{t'} - \mathbb{1}_G^{\mathrm{T}}P_{\circ}),\ t' \in \mathcal{T}_{t_0}^{\mathrm{S}}, \tag{17}$$
$$\widetilde{P}_{t'}^{\mathrm{r}} = \pi\widetilde{\xi}_{t'},\ t' \in \mathcal{T}_{t_0}^{\mathrm{S}}, \tag{18}$$

where $P_{\circ}$ is the *deterministic* dispatch decision and so only contributes to the nominal value of $P_{t'}^{\mathrm{r}}$.

With the above in place, we focus on (15)–(16) modelling the uncertain components of dynamic state variables. Substituting (18) into (15) then combining the resultant with (16) yields the following linear *time-varying* dynamical system:

$$\begin{bmatrix}\Delta\widetilde{\omega}_{t+\Delta t^{\mathrm{D}}}\\ \widetilde{P}^{\mathrm{m}}_{t+\Delta t^{\mathrm{D}}}\\ \widetilde{\xi}_{t+\Delta t^{\mathrm{D}}}\end{bmatrix} = \widetilde{A}_t\begin{bmatrix}\Delta\widetilde{\omega}_t\\ \widetilde{P}^{\mathrm{m}}_t\\ \widetilde{\xi}_t\end{bmatrix} + \widetilde{B}_t\widetilde{P}_t^{\mathrm{load}},\ t \in \mathcal{T}_{t_0}^{\mathrm{D}} \setminus \{t_0+T\}, \tag{19}$$

where matrices $\widetilde{A}_t$ and $\widetilde{B}_t$ are given by

$$\widetilde{A}_t = \left[\begin{array}{cc|c} & & \\ & A & \mathcal{O}_t C\pi \\ & & \\ \hline \mathcal{O}_t c & \mathbb{0}_G^{\mathrm{T}} & \mathcal{K}_t a\end{array}\right],\ \widetilde{B}_t = \left[\begin{array}{c} \\ B \\ \\ \hline \mathcal{O}_t b\end{array}\right], \tag{20}$$

with $\mathcal{K}_t = 1$ if $t \in \mathcal{T}_{t_0}^{\mathrm{S}}$ and $\mathcal{K}_t = 1/a$ otherwise.

We characterize $\{\widetilde{P}_t^{\mathrm{load}}\}_{t\in\mathcal{T}_{t_0}^{\mathrm{D}}}$ as independent Gaussian random variables with zero mean and standard deviation σ_t^{load}, i.e., $\widetilde{P}_t^{\mathrm{load}} \sim \mathcal{N}(0, (\sigma_t^{\mathrm{load}})^2)$. Since (19) is a linear system, we can propagate the uncertainty in $\{\widetilde{P}_t^{\mathrm{load}}\}_{t\in\mathcal{T}_{t_0}^{\mathrm{D}}}$ and model $\Delta\widetilde{\omega}_t$, $\widetilde{P}_t^{\mathrm{m}}$, and $\widetilde{\xi}_t$ by a joint Gaussian distribution with zero mean and covariance matrix $\Sigma_t \in \mathbb{R}^{(G+2)\times(G+2)}$, namely

$$\begin{bmatrix}\Delta\widetilde{\omega}_t & (\widetilde{P}_t^{\mathrm{m}})^{\mathrm{T}} & \widetilde{\xi}_t\end{bmatrix}^{\mathrm{T}} \sim \mathcal{N}\left(\mathbb{0}_{G+2}, \Sigma_t\right),\ t \in \mathcal{T}_{t_0}^{\mathrm{D}}. \tag{21}$$

Above, Σ_t can be evaluated in closed form as

$$\Sigma_t = \sum_{\upsilon=t_0}^{t-\Delta t^{\mathrm{D}}} (\Psi_{t,\upsilon+\Delta t^{\mathrm{D}}}\widetilde{B}_{\upsilon})(\sigma_{\upsilon}^{\mathrm{load}})^2(\Psi_{t,\upsilon+\Delta t^{\mathrm{D}}}\widetilde{B}_{\upsilon})^{\mathrm{T}}, \tag{22}$$

where the state transition matrix $\Psi_{t,\upsilon+\Delta t^{\mathrm{D}}}$ is given by

$$\Psi_{t,\upsilon+\Delta t^{\mathrm{D}}} = \begin{cases} \prod_{\upsilon+\Delta t^{\mathrm{D}}}^{t-\Delta t^{\mathrm{D}}} \widetilde{A}_{\upsilon+\Delta t^{\mathrm{D}}}, & \upsilon \in \{t_0, \ldots, t-2\Delta t^{\mathrm{D}}\}, \\ \mathrm{diag}(\mathbb{1}_{G+2}), & \upsilon = t - \Delta t^{\mathrm{D}}. \end{cases} \tag{23}$$

The initial condition $\Sigma_{t_0} = \mathbb{0}_{(G+2)\times(G+2)}$ since the corresponding state variables are assumed to be known precisely, i.e., with full certainty, at time t_0. At the expense of greater notational burden, the uncertainty propagation procedure above extends easily to accommodate correlation amongst different time samples of the net-load forecast by modelling the vector variable $[\{\widetilde{P}_t^{\text{load}}\}_{t\in\mathcal{T}_{t_0}^{\text{D}}}]$ as a multivariate Gaussian distribution with nonzero off-diagonal entries in its covariance matrix.

Key to reformulating the CCED in (6) into a computationally tractable deterministic optimization problem is to notice that the uncertainty in dynamic state variables can be fully characterized *before* solving the problem in (6). This is because the Gaussian distribution in (21) depends only on the uncertainty in the net-load forecast across the scheduling horizon along with system dynamics described by time-varying matrices $\widetilde{A}_t$ and $\widetilde{B}_t$, but *not* the optimal decisions of (6). For the deterministic reformulation outlined next, we will find it helpful to decompose the covariance matrix Σ_t into constituent blocks associated with dynamic state variables as

$$\Sigma_t := \begin{bmatrix} (\sigma_t^{\omega})^2 & \Sigma_t^{\omega,P} & \Sigma_t^{\omega,\xi} \\ \Sigma_t^{P,\omega} & \Sigma_t^{P} & \Sigma_t^{P,\xi} \\ \Sigma_t^{\xi,\omega} & \Sigma_t^{\xi,P} & (\sigma_t^{\xi})^2 \end{bmatrix}, \tag{24}$$

where all submatrices are suitably sized, e.g., $\Sigma_t^P \in \mathbb{R}^{G\times G}$.

C. Deterministic Problem Reformulation

Consider a typical quadratic cost function

$$C(P_t^{\text{m}}) = P_t^{\text{m}\,\text{T}}\text{diag}(q)P_t^{\text{m}} + r^{\text{T}}P_t^{\text{m}} + \mathbb{1}_G^{\text{T}}d, \tag{25}$$

where $q = [q_1, \ldots, q_G]^{\text{T}}$, $r = [r_1, \ldots, r_G]^{\text{T}}$, and $d = [d_1, \ldots, d_G]^{\text{T}}$ respectively represent its quadratic-, linear-, and constant-term coefficients. Now, bearing in mind that generator dynamic mechanical power trajectories are decomposed into nominal and uncertain components as in (9), we can express the objective function in (6a) as

$$\sum_{t\in\mathcal{T}_{t_0}^{\text{D}}} \big(C(\overline{P}_t^{\text{m}}) + (\sigma_t^P)^{\text{T}}\text{diag}(q)\sigma_t^P\big)\Delta t^{\text{D}}, \tag{26}$$

which holds given that the uncertain components are modelled by the Gaussian distribution in (21) with $\sigma_t^P \in \mathbb{R}^G$ denoting the element-wise square root of the vector of diagonal entries in Σ_t^P. In other words, each entry in σ_t^P represents the standard deviation of the marginal distribution of the uncertainty in the corresponding generator's mechanical power.

Critical in reformulating the dynamics-aware CCED in (6) into a deterministic problem is the ability to evaluate Σ_t in closed form with (22), rendering Σ_t *independent* of the optimal decisions solved from (6). Using this fact along with the updated objective function in (26), we reformulate the dynamic-aware CCED in (6) into the following computationally tractable deterministic counterpart:

$$\underset{\overline{\Omega}}{\text{minimize}} \sum_{t\in\mathcal{T}_{t_0}^{\text{D}}} \Big(C(\overline{P}_t^{\text{m}}) + (\sigma_t^P)^{\text{T}}\text{diag}(q)\sigma_t^P\Big)\Delta t^{\text{D}} \tag{27a}$$

$$\text{subject to } M_{\text{eff}}\Big(\frac{\Delta\overline{\omega}_{t+\Delta t^{\text{D}}} - \Delta\overline{\omega}_t}{\Delta t^{\text{D}}}\Big) = \mathbb{1}_G^{\text{T}}\overline{P}_t^{\text{m}} - D_{\text{eff}}\Delta\overline{\omega}_t - \overline{P}_t^{\text{load}},\ (\alpha_t),\ t\in\mathcal{T}_{t_0}^{\text{D}}\setminus\{t_0+T\}, \tag{27b}$$

$$\tau\Big(\frac{\overline{P}_{t+\Delta t^{\text{D}}}^{\text{m}} - \overline{P}_t^{\text{m}}}{\Delta t^{\text{D}}}\Big) = \overline{P}_{t'}^{\text{r}} - \overline{P}_t^{\text{m}} - R^{-1}\mathbb{1}_G\Delta\overline{\omega}_t,\ (\eta_t),\ t'\in\mathcal{T}_{t_0}^{\text{S}}\setminus\{t_0+T\},\ t\in\{t',\ldots,t'+\Delta t^{\text{S}}-\Delta t^{\text{D}}\}, \tag{27c}$$

$$\tau_{\text{A}}\Big(\frac{\overline{\xi}_{t'+\Delta t^{\text{S}}} - \overline{\xi}_{t'}}{\Delta t^{\text{S}}}\Big) = -\overline{\xi}_{t'} + k\beta\Delta\overline{\omega}_{t'} + \overline{P}_{t'}^{\text{load}},\ (\gamma_{t'}),\ t'\in\mathcal{T}_{t_0}^{\text{S}}\setminus\{t_0+T\}, \tag{27d}$$

$$\overline{P}_{t'}^{\text{r}} = P_\circ + \pi(\overline{\xi}_{t'} - \mathbb{1}_G^{\text{T}}P_\circ),\ (\kappa_{t'}),\ t'\in\mathcal{T}_{t_0}^{\text{S}}, \tag{27e}$$

$$\mathbb{1}_G^{\text{T}}P_\circ = \frac{1}{|\mathcal{T}_{t_0}^{\text{D}}|}\sum_{t\in\mathcal{T}_{t_0}^{\text{D}}}\overline{P}_t^{\text{load}},\ (\zeta), \tag{27f}$$

$$\Delta\overline{\omega}_t + \sigma_t^{\omega}\Phi^{-1}(1-\varepsilon^{\omega}) \le \Delta\omega_{\max},\ (\rho_t^+),\ t\in\mathcal{T}_{t_0}^{\text{D}}, \tag{27g}$$

$$\Delta\overline{\omega}_t - \sigma_t^{\omega}\Phi^{-1}(1-\varepsilon^{\omega}) \ge \Delta\omega_{\min},\ (\rho_t^-),\ t\in\mathcal{T}_{t_0}^{\text{D}}, \tag{27h}$$

$$\overline{P}_t^{\text{m}} + \sigma_t^P\Phi^{-1}(1-\varepsilon^P) \le P_{\max}^{\text{m}},\ (\mu_t^+),\ t\in\mathcal{T}_{t_0}^{\text{D}}, \tag{27i}$$

$$\overline{P}_t^{\text{m}} - \sigma_t^P\Phi^{-1}(1-\varepsilon^P) \ge P_{\min}^{\text{m}},\ (\mu_t^-),\ t\in\mathcal{T}_{t_0}^{\text{D}}, \tag{27j}$$

where $\overline{\Omega} = \{P_\circ, \Delta\overline{\omega}_t, \overline{P}_t^{\text{m}}, \overline{P}_{t'}^{\text{r}}, \overline{\xi}_{t'}\}_{t\in\mathcal{T}_{t_0}^{\text{D}},\, t'\in\mathcal{T}_{t_0}^{\text{S}}}$ collects decision variables of the reformulated deterministic problem with quadratic cost and linear constraints that can be solved at scale using off-the-shelf optimization packages. Above, (27g)–(27j) are deterministic constraints reformulated from chance constraints in (6g)–(6j), where the required reserve margins are informed by the uncertainty in associated dynamic decision variables (quantified by σ_t^{ω} and σ_t^P) subject to tolerable risk of violating their limits (imposed by ε^{ω} and ε^P), with $\Phi^{-1}(\cdot)$ denoting the inverse of the cumulative distribution function of the standard Gaussian distribution.

Remark 2 (Non-Gaussian Uncertainty)**.** For more general non-Gaussian net-load uncertainty, approaches to reformulate a CCED into a deterministic problem include using non-parametric probability distributions [31], Gaussian mixtures models [32], and first and second moments of a family of distributions estimated from empirical data [33]. These methods can be applied to solve the dynamics-aware CCED formulated in (6) in a straightforward manner at the expense of potentially greater complexity to reformulate the chance-constrained optimization problem into an equivalent or approximate deterministic counterpart and subsequent computational burden to solve it. ■

Remark 3 (Joint Double-sided Chance Constraints)**.** Our approach to reformulating the CCED into a deterministic problem follows prior work in [34]–[36], where joint double-sided chance constraints are approximated using less conservative separate single-sided constraints. This approximation simplifies the problem reformulation and facilitates subsequent solution tractability. At the same time, we note that chance-constrained problems embedding joint two-sided chance constraints can still be reformulated into deterministic counterparts using various other approximations [37]–[39]. Moreover, there is flexibility in the problem formulated in (6) for a

system operator to enforce varying risk profiles by adjusting the tuneable parameters ε^{ω} and ε^{P} representing the tolerable probability of violating separate single-sided limits. ■

Before deriving the dynamics-aware price of reserves in the next section, we express the Lagrangian of the deterministic reformulation of the dynamics-aware CCED in (27) as

$$\begin{aligned}
\mathcal{L} = &\sum_{t\in\mathcal{T}^{\mathrm{D}}_{t_0}} \Big(\Big(C(\overline{P}^{\mathrm{m}}_t) + (\sigma^P_t)^{\mathrm{T}} \mathrm{diag}(q) \sigma^P_t \Big) \Delta t^{\mathrm{D}} \\
&+ \rho^{+}_t \big(\Delta\overline{\omega}_t + \sigma^{\omega}_t \Phi^{-1}(1-\varepsilon^{\omega}) - \Delta\omega_{\max} \big) \\
&+ \rho^{-}_t \big(\Delta\omega_{\min} - \Delta\overline{\omega}_t + \sigma^{\omega}_t \Phi^{-1}(1-\varepsilon^{\omega}) \big) \\
&+ \mu^{+\mathrm{T}}_t \big(\overline{P}^{\mathrm{m}}_t + \sigma^P_t \Phi^{-1}(1-\varepsilon^P) - P^{\mathrm{m}}_{\max} \big) \\
&+ \mu^{-\mathrm{T}}_t \big(P^{\mathrm{m}}_{\min} - \overline{P}^{\mathrm{m}}_t + \sigma^P_t \Phi^{-1}(1-\varepsilon^P) \big) \Big) \\
&+ \sum_{t'\in\mathcal{T}^{\mathrm{S}}_{t_0}} \kappa^{\mathrm{T}}_{t'} (\overline{P}^{\mathrm{r}}_{t'} - P_{\circ} - \pi(\overline{\xi}_{t'} - \mathbb{1}^{\mathrm{T}}_G P_{\circ})) \\
&+ \sum_{t\in\mathcal{T}^{\mathrm{D}}_{t_0}\setminus\{t_0+T\}} \Big(\alpha_t \Big(M_{\mathrm{eff}} \Big(\frac{\Delta\overline{\omega}_{t+\Delta t^{\mathrm{D}}} - \Delta\overline{\omega}_t}{\Delta t^{\mathrm{D}}} \Big) - \mathbb{1}^{\mathrm{T}}_G \overline{P}^{\mathrm{m}}_t \\
&\quad + D_{\mathrm{eff}} \Delta\overline{\omega}_t + \overline{P}^{\mathrm{load}}_t \Big) + \eta^{\mathrm{T}}_t \Big(\tau \Big(\frac{\overline{P}^{\mathrm{m}}_{t+\Delta t^{\mathrm{D}}} - \overline{P}^{\mathrm{m}}_t}{\Delta t^{\mathrm{D}}} \Big) \\
&\quad - P^{\mathrm{r}}_{t'} + \overline{P}^{\mathrm{m}}_t + R^{-1} \mathbb{1}_G \Delta\overline{\omega}_t \Big) \Big) \\
&+ \sum_{t'\in\mathcal{T}^{\mathrm{S}}_{t_0}\setminus\{t_0+T\}} \gamma_{t'} \Big(\tau_{\mathrm{A}} \Big(\frac{\overline{\xi}_{t'+\Delta t^{\mathrm{S}}} - \overline{\xi}_{t'}}{\Delta t^{\mathrm{S}}} \Big) + \overline{\xi}_{t'} - k\beta\Delta\overline{\omega}_{t'} - \overline{P}^{\mathrm{load}}_{t'} \Big) \\
&+ \zeta \Big(\frac{1}{|\mathcal{T}^{\mathrm{D}}_{t_0}|} \sum_{t\in\mathcal{T}^{\mathrm{D}}_{t_0}} \overline{P}^{\mathrm{load}}_t - \mathbb{1}^{\mathrm{T}}_G P_{\circ} \Big). \qquad (28)
\end{aligned}$$

We introduce notation for the optimal Lagrangian as $\mathcal{L}^{\star}$ and the optimal decisions of the problem in (27) as $\overline{\Omega}^{\star} = \{P^{\star}_{\circ}, \Delta\overline{\omega}^{\star}_t, \overline{P}^{\mathrm{m}\star}_t, \overline{P}^{\mathrm{r}\star}_{t'}, \overline{\xi}^{\star}_{t'}\}_{t\in\mathcal{T}^{\mathrm{D}}_{t_0}, t'\in\mathcal{T}^{\mathrm{S}}_{t_0}}$. Also let Lagrange multipliers evaluated at the optimal solution be distinguished with superscript $\star$. For example, $\mu^{+\star}_t$ and $\mu^{-\star}_t$ respectively refer to values taken by μ^{+}_t and μ^{-}_t at the optimal solution.

IV. Dynamics-aware Price of Reserves

The paper's main results outlined in this section relate to the dynamics-aware price of reserves defined as the system marginal operation cost due to an incremental change in the net-load uncertainty while satisfying dynamic constraints.

Theorem 1. Given the optimal Lagrangian $\mathcal{L}^{\star}$ of the dynamics-aware CCED after being reformulated into a deterministic problem, i.e., the problem in (27), and its optimal solution $\{P^{\star}_{\circ}, \Delta\overline{\omega}^{\star}_t, \overline{P}^{\mathrm{m}\star}_t, \overline{P}^{\mathrm{r}\star}_{t'}, \overline{\xi}^{\star}_{t'}\}_{t\in\mathcal{T}^{\mathrm{D}}_{t_0}, t'\in\mathcal{T}^{\mathrm{S}}_{t_0}}$, the dynamics-aware price of reserves at time $t \in \mathcal{T}^{\mathrm{D}}_{t_0}$ is expressed as

$$\begin{aligned}
\Lambda^{\star}_t = &\frac{1}{\Delta t^{\mathrm{D}}} \sum_{v\in\mathcal{T}^{\mathrm{D}}_{t+\Delta t^{\mathrm{D}}}} \Phi^{-1}(1-\varepsilon^{\omega}) (\rho^{+\star}_v + \rho^{-\star}_v) \frac{\partial\sigma^{\omega}_v}{\partial\sigma^{\mathrm{load}}_t} \\
&+ \frac{1}{\Delta t^{\mathrm{D}}} \sum_{v\in\mathcal{T}^{\mathrm{D}}_{t+\Delta t^{\mathrm{D}}}} \Phi^{-1}(1-\varepsilon^{P}) (\mu^{+\star}_v + \mu^{-\star}_v)^{\mathrm{T}} \frac{\partial\sigma^{P}_v}{\partial\sigma^{\mathrm{load}}_t} \\
&+ \sum_{v\in\mathcal{T}^{\mathrm{D}}_{t+\Delta t^{\mathrm{D}}}} 2(\sigma^P_v)^{\mathrm{T}} \mathrm{diag}(q) \frac{\partial\sigma^{P}_v}{\partial\sigma^{\mathrm{load}}_t}, \qquad (29)
\end{aligned}$$

where $\mathcal{T}^{\mathrm{D}}_{t+\Delta t^{\mathrm{D}}} = \{t+\Delta t^{\mathrm{D}}, t+2\Delta t^{\mathrm{D}}, \ldots, t_0+T\}$, and $\frac{\partial\sigma^{\omega}_v}{\partial\sigma^{\mathrm{load}}_t}$ and $\frac{\partial\sigma^{P}_v}{\partial\sigma^{\mathrm{load}}_t}$ are, respectively, the first and next G entries of

$$\frac{1}{2} (\mathrm{diag}(\Sigma_v))^{-\frac{1}{2}} \frac{\partial \mathrm{diag}(\Sigma_v)}{\partial\sigma^{\mathrm{load}}_t} \cdot \mathbb{1}_{G+2}, \qquad (30)$$

and $\mathrm{diag}(\Sigma_v)$ denotes a diagonal matrix containing entries in the main diagonal of Σ_v and zeros elsewhere.

Proof. The price of reserves can be defined as the sensitivity of the optimal Lagrangian with respect to uncertainty in the net-load forecast [11], [12]. In our case, this uncertainty is quantified by the standard deviation of the net-load forecast σ^{load}_t, $t \in \mathcal{T}^{\mathrm{D}}_{t_0}$, so the dynamics-aware price of reserves is expressed as the following derivative of the optimal Lagrangian:

$$\Lambda^{\star}_t := \frac{1}{\Delta t^{\mathrm{D}}} \frac{\partial\mathcal{L}^{\star}}{\partial\sigma^{\mathrm{load}}_t}, \; t \in \mathcal{T}^{\mathrm{D}}_{t_0}, \qquad (31)$$

where dividing by Δt^{D} yields units consistent with the cost function. Via visual inspection of (28) in conjunction with (22), we see that $\mathcal{L}^{\star}$ is related to σ^{load}_t through σ^{ω}_v and σ^{P}_v, $v \in \mathcal{T}^{\mathrm{D}}_{t+\Delta t^{\mathrm{D}}}$. Thus, applying the chain rule in calculus, (31) evaluates as

$$\Lambda^{\star}_t = \frac{1}{\Delta t^{\mathrm{D}}} \sum_{v\in\mathcal{T}^{\mathrm{D}}_{t+\Delta t^{\mathrm{D}}}} \Big(\frac{\partial\mathcal{L}^{\star}}{\partial\sigma^{\omega}_v} \frac{\partial\sigma^{\omega}_v}{\partial\sigma^{\mathrm{load}}_t} + \Big(\frac{\partial\mathcal{L}^{\star}}{\partial\sigma^{P}_v} \Big)^{\mathrm{T}} \frac{\partial\sigma^{P}_v}{\partial\sigma^{\mathrm{load}}_t} \Big), \qquad (32)$$

which then yields (29) via straightforward differentiation of (28) followed by algebraic manipulation of the resultant. Next, to get $\frac{\partial\sigma^{\omega}_v}{\partial\sigma^{\mathrm{load}}_t}$ and $\frac{\partial\sigma^{P}_v}{\partial\sigma^{\mathrm{load}}_t}$ needed in (29), we recognize from the variables defined in (24) that

$$\frac{\partial}{\partial\sigma^{\mathrm{load}}_t} \begin{bmatrix} \sigma^{\omega}_v \\ \sigma^{P}_v \\ \sigma^{\xi}_v \end{bmatrix} = \frac{\partial (\mathrm{diag}(\Sigma_v))^{\frac{1}{2}}}{\partial\sigma^{\mathrm{load}}_t} \cdot \mathbb{1}_{G+2}, \qquad (33)$$

the right-hand side of which evaluates as (30) via direct differentiation followed by the chain rule in calculus. □

We next highlight key characteristics of the dynamics-aware price of reserves as expressed in (29):

i) Similar to the solution of the static CCED in (1), the dynamics-aware price of reserves internalizes uncertainty in decision variables and generator risk tolerance via explicit dependence on Σ_t and ε^{P}, respectively. Generalizing over its static counterpart, the dynamics-aware price additionally incorporates the uncertainty associated with dynamic state variables during the post-disturbance transients as well as in steady state.

ii) The dynamics-aware price of reserves further extends beyond conventional static alternatives with a term explicitly accounting for the risk of violating frequency limits during system transients prior to converging to steady state, thus offering a systematic approach to price generator reserves that contribute to de-risking dynamic frequency performance.

iii) The explicit dependence of the dynamics-aware price of reserves on Σ_t couples it with individual generator parameters that directly impact the system dynamic risk profile. Specifically, the closed-form expression for Σ_t

in (22) involves system matrices $\widetilde{A}_t$ and $\widetilde{B}_t$, $t \in \mathcal{T}^{\mathrm{D}}_{t_0}$, that in turn embed dynamic parameters of generators, i.e., M_g, D_g, τ_g, and R_g^{-1}, $g \in \mathcal{G}$, as well as the AGC, i.e., τ_{A}, k, and β. This feature is useful to incentivize inverter-based resources capable of modifying their controller parameters in support of dynamic frequency response.

iv) The dynamics-aware price of reserves at time t in (29) depends on *future* dynamics in both system uncertainty and Lagrange multipliers, occurring after time t. This is in contrast to the physical power system dynamics depending on the *past* before time t. Here, we can conclude that the price of reserves indeed serves to compensate generators for de-risking future performance.

Remark 4 (Non-binding Inequality Constraints)**.** We further note that entries of Lagrange multipliers $\rho_v^{+\star}$ or $\mu_v^{+\star}$ in (29) are nonzero only if upper limits for the corresponding system frequency or generator mechanical power chance constraints, respectively, are binding at time v, otherwise they are zero. The same holds for $\rho_v^{-\star}$ and $\mu_v^{-\star}$ related to lower limits. Now suppose the aforementioned inequality chance constraints are not binding at the optimal solution, so the first two summation terms in (29) yield exactly zero, and the price of reserves simplifies as the nonzero third term in (29) given by

$$\Lambda_t^\star = \sum_{v \in \mathcal{T}^{\mathrm{D}}_{t+\Delta t^{\mathrm{D}}}} 2(\sigma_v^P)^{\mathrm{T}} \mathrm{diag}(q) \frac{\partial \sigma_v^P}{\partial \sigma_t^{\mathrm{load}}}. \tag{34}$$

The quantity in (34) can be interpreted as the cost to re-dispatch reserves due to an incremental change in net-load uncertainty at time t, in the absence of binding generator power or system frequency inequality chance constraints. ■

A. Evaluating Dynamics-aware Reserve Revenue

The dynamics-aware price of reserves at time $t \in \mathcal{T}^{\mathrm{D}}_{t_0}$, $\Lambda_t^\star$, evaluates as (29) aided by (30). We further make use of the fact that $\frac{\partial \mathrm{diag}(\Sigma_v)}{\partial \sigma_t^{\mathrm{load}}} = \mathrm{diag}\Big(\frac{\partial \Sigma_v}{\partial \sigma_t^{\mathrm{load}}}\Big)$ to calculate $\frac{\partial \mathrm{diag}(\Sigma_v)}{\partial \sigma_t^{\mathrm{load}}}$ in (30) in closed form by taking the diagonal entries of

$$\frac{\partial \Sigma_v}{\partial \sigma_t^{\mathrm{load}}} = 2(\Psi_{v,t+\Delta t^{\mathrm{D}}} \widetilde{B}_t)\sigma_t^{\mathrm{load}} (\Psi_{v,t+\Delta t^{\mathrm{D}}} \widetilde{B}_t)^{\mathrm{T}}, \quad v \in \mathcal{T}^{\mathrm{D}}_{t+\Delta t^{\mathrm{D}}}, \tag{35}$$

i.e., the derivative of (22). Given the dynamics-aware price of reserves $\Lambda_t^\star$, we calculate the generator reserve revenue as

$$\sum_{t \in \mathcal{T}^{\mathrm{D}}_{t_0}} \Lambda_t^\star \sigma_t^P \Delta t^{\mathrm{D}}, \tag{36}$$

where σ_t^P is obtained in closed form from (22) as the element-wise square root of the vector of diagonal entries in Σ_t^P.

Example 2 (WSCC 3-Generator Test System)**.** Using the same test system as in Example 1, we consider a scheduling horizon starting from time $t_0 = 0\,[\mathrm{sec}]$ of length $T = 90\,[\mathrm{sec}]$ (i.e., $1.5\,[\mathrm{min}]$). Shorter time intervals of length $\Delta t^{\mathrm{D}} = 0.05\,[\mathrm{sec}]$[1] capture faster frequency dynamics. Then longer time intervals are set to $\Delta t^{\mathrm{S}} = \Delta t^{\mathrm{D}}$ rendering $\mathcal{T}^{\mathrm{S}}_{t_0} = \mathcal{T}^{\mathrm{D}}_{t_0}$, in accordance with Proposition 1 in [22]. Furthermore, Gaussian uncertainty in the net-load forecast is modelled with standard deviation $\sigma_t^{\mathrm{load}} = 0.15\,[\mathrm{p.u.}]$, $\forall\, t \in \mathcal{T}^{\mathrm{D}}_{t_0}$. The tolerable limits in the probability of violating chance constraints are set as $\varepsilon^P = 0.1$ and $\varepsilon^\omega = 0.1$. This tolerance may be set to meet certain system reliability criteria, such as expected energy not served [12]. Consistent with standard practice (see, e.g., [24], [26]), the area bias factor in the AGC is set as $\beta = \sum_{g \in \mathcal{G}} (D_g + R_g^{-1})$. Then, for each set of dynamic parameter values reported in Table I and with the upper limits of generator mechanical power as $P^{\mathrm{m}}_{\max} = [3, 2, 3]^{\mathrm{T}}\,[\mathrm{p.u.}]$, we model the problem in (27) in the MATLAB YALMIP toolbox and solve it using MOSEK.

[1] Via simulations of standard test systems, we find that the choice of $\Delta t^{\mathrm{D}} = 0.05\,[\mathrm{sec}]$ adequately captures dynamics in the time-scales of our interest while containing computational burden of solving the CCED. Smaller or larger discretization intervals may be chosen to satisfy specific requirements in model accuracy or limitations in computational resources, respectively.

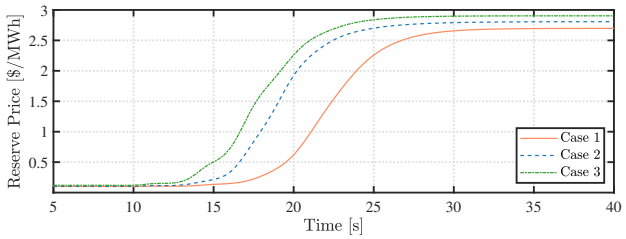

Fig. 2: (Example 2). Trajectories of the price of reserves obtained from optimal solution of the reformulated dynamics-aware CCED, i.e., (27), with dynamic parameter values given in Table I.

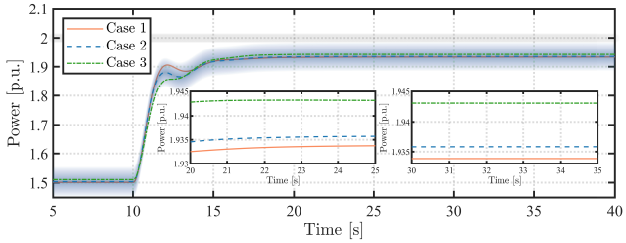

Fig. 3: (Example 2). Dynamic mechanical power trajectories for generator 2 realized with dynamic parameter values given in Table I. Individual traces represent the nominal (or mean) trajectories, which are associated with the Gaussian distribution given by (21) propagated from uncertainty in the net-load forecast. To illustrate concepts, the uncertainty distribution around the nominal trajectory is plotted as a translucent band for case 2 only, while those for the other two cases are omitted to promote clarity of the figure.

Given the optimal solution of (27), we evaluate the dynamics-aware price of reserves $\Lambda_t^\star$ using (29) in conjunction with (30) and (35) and plot their trajectories in Fig. 2. Prior to the load increase at time $t = 10\,[\mathrm{sec}]$, the price takes a small nonzero value equal to the third term in (29). Following the load increase, the chance constraint pertaining to the upper limit of generator 2 mechanical power becomes binding. The gap observed between the nominal trajectories and the limit of $2\,[\mathrm{p.u.}]$ in Fig. 3 constitutes the reserve margin required to satisfy the pertinent chance constraint. This leads to the increase in the price of reserves, as shown in Fig. 2. The price of reserves then converges to steady state alongside the nominal trajectories of the dynamic state variables, as comparison of the zoomed portions in Fig. 3 illustrates. Both the dynamics-aware price of reserves and the subsequent total reserve revenue, calculated using (36) and plotted in Fig. 4, increase from case 1 to 3, consistent with the trend of improved system dynamic risk profile highlighted in Example 1. Also

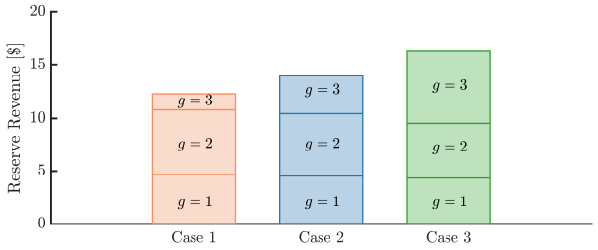

Fig. 4: (Example 2). Total reserve revenue shared amongst the three generators for dynamic parameter values given in Table I.

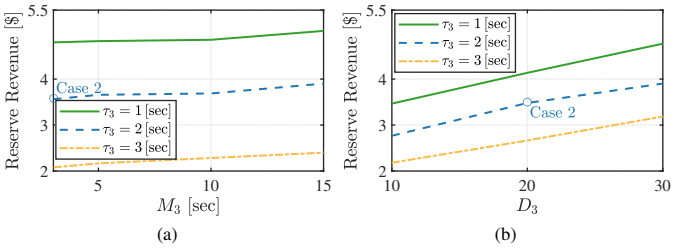

Fig. 5: (Example 3). Dynamics-aware reserve revenue for generator 3 with different values taken by its (a) inertia constant M_3 and (b) damping constant D_3, and parameterized by its turbine-governor time constant τ_3. The $\circ$ symbols represent the revenues given parameter values in case 2 from Table I.

increasing from case 1 to 3 is the individual reserve revenue for generator 3 because it is exposed to greater uncertainty (and thus risk of violating its generation limits) with its changing parameter values, as shown in Fig. 1a. Conversely, individual reserve revenues for generators 1 and 2 decrease as they are exposed to lower uncertainty and risk. ■

B. Assessing Impact of Varying Dynamic Parameter Values

The dynamics-aware price of reserves in (29) internalizes uncertainty in decision variables via its dependence on Σ_t and $\frac{\partial \mathrm{diag}(\Sigma_\upsilon)}{\partial \sigma_t^{\mathrm{load}}}$, $t \in \mathcal{T}_{t_0}^{\mathrm{D}}$, $\upsilon \in \mathcal{T}_{t+\Delta t^{\mathrm{D}}}^{\mathrm{D}}$, evaluated in closed form via (22) and (35), respectively. Visual inspection of these closed-form expressions reveals that they, in turn, depend on system matrices $\widetilde{A}_t$ and $\widetilde{B}_t$, $t \in \mathcal{T}_{t_0}^{\mathrm{D}}$, that embed generator dynamic parameters M_g, D_g, τ_g, and R_g^{-1}, $g \in \mathcal{G}$, as well as AGC parameters τ_{A}, k, and β. This explicit dependence is critical to couple the pricing of reserves with individual generator contributions to system dynamic risk profile subject to industry-standard primary and secondary frequency controls. Via a numerical example, we next illustrate how values taken by dynamic parameters of a generator affect its reserve revenue under the proposed dynamics-aware pricing of reserves.

Example 3 (WSCC 3-Generator Test System)**.** Revisiting the test system and simulation setup from Example 2, we repeatedly calculate the dynamics-aware reserve revenue available to generator 3 under different values taken by M_3, D_3, and τ_3, while fixing parameter values for generators 1 and 2 to those reported for case 2 in Table I. In Fig. 5, greater reserve revenue for generator 3, shown as green-colour traces, are associated with faster primary frequency response made possible by smaller value taken by τ_3, while orange-colour traces represent lower revenue for generator 3 offering slower primary frequency response. Furthermore, parameterizing with respect to τ_3 in Fig. 5a, setting M_3 to larger values provides generator 3 with greater reserve revenue, commensurate with its contribution to inertial response immediately after a disturbance. Similarly, in Fig. 5b, larger values taken by D_3 are associated with greater reserve revenue to compensate generator 3 for contributing to improvements in transient frequency damping. ■

V. Case Studies

This section presents detailed numerical case studies involving the WSCC test system [30]. They demonstrate improved system dynamic performance and greater generator revenues resulting from the proposed method when compared to the solution of the static CCED in (1), dynamics-aware reserve revenue adequacy for the system, and cost recovery for each generator. Further demonstrated via numerical simulations involving the New England test system [40] is the computational scalability of the proposed approach.

A. Dynamic Performance

We modify the simulation setup from Example 2 by setting generator dynamic parameters to their default values provided in Table I as case 2. The cost of generation across the scheduling horizon of length $T = 300\,[\mathrm{sec}]$ (i.e., $5\,[\mathrm{min}]$) is given by

$$C(P_t^{\mathrm{m}}) = (P_t^{\mathrm{m}})^{\mathrm{T}} \mathrm{diag}(\begin{bmatrix}0.22 & 0.085 & 0.6125\end{bmatrix}) P_t^{\mathrm{m}} + \begin{bmatrix}5 & 1.2 & 5\end{bmatrix} P_t^{\mathrm{m}},\ t \in \mathcal{T}_{t_0}^{\mathrm{D}}. \tag{37}$$

We impose several step changes in the nominal net-load forecast, as shown in Fig. 6, consisting of an increase by 15% at time $t = 20\,[\mathrm{sec}]$, followed by decreases of 5% and 10% at times $t = 60\,[\mathrm{sec}]$ and $t = 80\,[\mathrm{sec}]$, respectively, and a subsequent increase of 15% at time $t = 100\,[\mathrm{sec}]$ then constant thereafter. Similar to Example 2, uncertainty in the net load is modelled as a Gaussian distribution. The maximum power limit for generator 2 is again set to be $2\,[\mathrm{p.u.}]$. The corresponding chance constraint becomes binding from $t = 20\,[\mathrm{sec}]$ to $t = 60\,[\mathrm{sec}]$ and again after $t = 100\,[\mathrm{sec}]$ consistent with larger net-load forecast values during these periods.

1) Price of Reserves: We use (29) to evaluate the dynamics-aware price of reserves at the optimal solution of the problem in (27) subject to various levels of net-load forecast uncertainty and tolerable probability of chance constraint violation. The resulting prices of reserves are plotted in Fig. 7. Particularly, in Fig. 7a, greater net-load forecast uncertainty realized with larger standard deviation values results in higher price of reserves, commensurate with the greater subsequent risk undertaken by generators in potentially violating their operational limits. Related to this, as shown in Fig. 7b, lower level of risk of violating operational limits tolerated by generators yields higher price of reserves, consistent with improved ability to de-risk system dynamic performance under uncertainty.

2) Generator Mechanical Powers: As shown in Fig. 8, generator 2 increases its production in response to the net-load increases imposed at times $t = 20$ and $t = 100\,[\mathrm{sec}]$. We observe that the mechanical power trajectory and its uncertainty distribution (highlighted in purple colour) solved from the

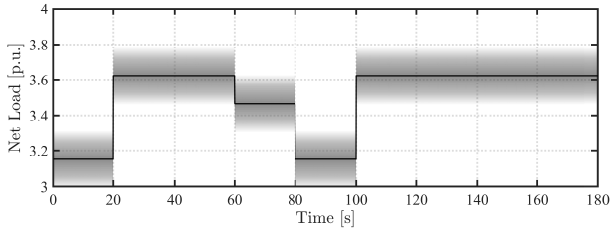

Fig. 6: System net-load forecast profile with uncertainty distribution plotted as a translucent band around the nominal trajectory.

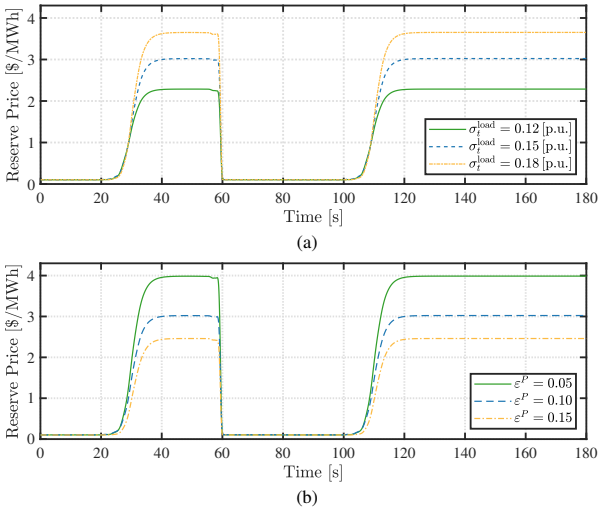

Fig. 7: Price of reserves evaluated at the optimal solution of the problem in (27) subject to various levels of (a) net-load uncertainty and (b) generator risk tolerance, quantified respectively by standard deviation of the forecast uncertainty σ_t^{load}, $t \in \mathcal{T}_{t_0}^{\text{D}}$, and tolerable probability of violating generation limits ε^P.

dynamics-aware CCED satisfy the chance constraint pertinent to generator 2's maximum power limit. For comparison, we apply the optimal set-points solved from the static CCED in (1) with the initial load forecast as the generator references in a dynamic simulation performed in PSAT [41]. Custom MATLAB code augmenting the standard PSAT toolbox implements the AGC to regulate system frequency, the model for which is described in Section II-B. Plotted in orange colour in Fig. 8, the resulting dynamic mechanical power trajectory and associated uncertainty distribution patently violate the maximum generation limit for a considerable amount of time.

B. Costs, Revenues, and Profits

We calculate costs, revenues, and profits realized from the proposed dynamics-aware price of reserves and i) compare them to the solution of the static counterpart in (1), ii) assess system reserve revenue adequacy, and iii) verify cost recovery for each generator. To offer comparisons over a broader range of scenarios, we consider four nominal net-load profiles that all begin with the same initial value as in Fig. 6 but then each followed by $90\%, 100\%$, 110%, and 120% of the variations described in Section V-A at times $t = 20$, 60, 80, and 100 [sec].

1) Total Across All Generators: The total dynamics-aware revenue is calculated as

$$\sum_{t\in\mathcal{T}_{t_0}^{\text{D}}} \Big(\frac{1}{\Delta t^{\text{D}}}\frac{\partial \mathcal{L}^\star}{\partial \overline{P}_t^{\text{load}}}\Big)\overline{P}_t^{\text{load}}\Delta t^{\text{D}} + \sum_{t\in\mathcal{T}_{t_0}^{\text{D}}} \Lambda_t^\star \mathbb{1}_G^{\text{T}} \sigma_t^P \Delta t^{\text{D}}, \quad (38)$$

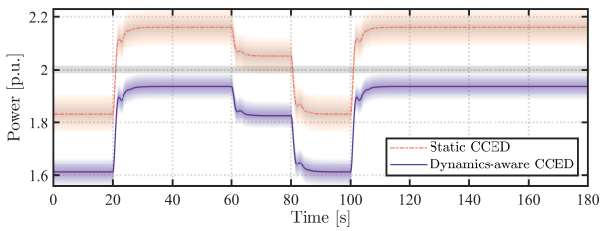

Fig. 8: Time-domain mechanical power trajectories of generator 2, for which the maximum limit is 2 [p.u.], realized with the static and dynamics-aware CCED set-points. Uncertainty distributions are plotted as translucent bands.

TABLE II: Total generator revenues, costs, and profits realized from static and dynamics-aware CCEDs for various levels of changes in forecasted loads.

Percentage of Load Profile		90%	100%	110%	120%
Revenue [$]	Static	583.8	608.5	636.4	665.0
	Dynamics-aware	802.4	832.7	860.3	899.2
Cost [$]	Static	384.1	395.4	407.6	423.8
	Dynamics-aware	497.6	512.6	528.1	548.3
Profit [$]	Static	199.7	213.1	228.8	241.2
	Dynamics-aware	304.8	320.1	332.2	350.9

where the second term represents reserve revenue evaluated as the sum of all entries of (36) and the first term is the revenue for energy produced with corresponding price $\frac{1}{\Delta t^{\text{D}}}\frac{\partial \mathcal{L}^\star}{\partial \overline{P}_t^{\text{load}}}$ obtained via straightforward differentiation of the optimal Lagrangian in (28) (see, e.g., [22]). To calculate the cost of generation, we consider the average value given by

$$\sum_{t\in\mathcal{T}_{t_0}^{\text{D}}} C(\overline{P}_t^{\text{m}\star})\Delta t^{\text{D}}. \quad (39)$$

Quantities needed to evaluate (38) and (39), namely the nominal generator mechanical power $\overline{P}_t^{\text{m}\star}$, its uncertainty distribution quantified by σ_t^P, and dynamics-aware price of reserves $\Lambda_t^\star$, all accompany the optimal solution of the problem in (27), i.e., the deterministic reformulation of the dynamics-aware CCED. The difference between the revenue in (38) and the cost in (39) represents the total profit. We also solve the deterministic reformulation of the problem in (1) subject to the initial load forecast to obtain the dynamics-oblivious prices of reserves and energy. The corresponding optimal generator set-points are applied to a PSAT simulation augmented with the AGC to yield mechanical power trajectories that are then used to calculate generation cost.

For each net-load forecast scenario, Table II reports total revenues, costs, and profits as the difference between the two. The dynamics-aware CCED solution indeed offers greater revenues for generators compared to its static counterpart as the dynamics-aware price of reserves $\Lambda_t^\star$ internalizes uncertainty in dynamic state variables (like system frequency and generator mechanical power) and acceptable levels of risk of violating their operational limits during transients. Meanwhile, greater costs in the dynamics-aware case can be attributed to the ability to de-risk dynamic performance during transients not possible under the steady-state assumption in the static CCED. To see this, consider as an example the mechanical power trajectories of generator 2 in Fig. 8. Here, decisions from the static CCED violate the maximum generation limit, whereas the dynamics-aware CCED solution satisfies the limit

TABLE III: Verifying dynamics-aware reserve revenue adequacy given various levels of changes in forecasted loads.

Percentage of Load Profile	90%	100%	110%	120%
Revenue from Customers [$]	39.2	41.2	42.3	44.5
Payment to Generators [$]	34.1	35.9	37.4	38.8

TABLE IV: Verifying cost recovery for all generators given various levels of changes in forecasted loads.

Percentage of Load Profile		90%	100%	110%	120%
$g = 1$	Revenue [$]	332.4	345.1	356.4	372.6
	Cost [$]	289.3	298.1	307.0	318.7
$g = 2$	Revenue [$]	414.5	430.3	444.5	464.6
	Cost [$]	158.5	163.3	168.2	174.5
$g = 3$	Revenue [$]	55.1	57.2	59.1	61.8
	Cost [$]	49.7	51.3	52.8	54.8

at the cost of increasing the dispatch from the other two more expensive generators. Finally, although the dynamics-aware CCED leads to greater costs of generation (on average), these are not as significant as the gains in revenues on offer from the dynamics-aware pricing of reserves and energy in (38). In this way, the dynamics-aware pricing indeed serves to incentivize generators to de-risk system dynamic performance against greater net-load uncertainty and larger and more frequent transient excursions expected in future power systems.

2) System Revenue Adequacy: We evaluate revenue adequacy for the system operator to procure reserves by verifying that the total payment to all generators needed for reserves (i.e., the second term in (38)) satisfies

$$\sum_{t\in\mathcal{T}^{\mathrm{D}}_{t_0}} \Lambda^{\star}_t \mathbb{1}^{\mathrm{T}}_G \sigma^P_t \Delta t^{\mathrm{D}} \leq \sum_{t\in\mathcal{T}^{\mathrm{D}}_{t_0}} \Lambda^{\star}_t \sigma^{\mathrm{load}}_t \Delta t^{\mathrm{D}}, \tag{40}$$

where the right-hand side represents the revenue yielded from load serving entities (i.e., customers). As shown in Table III, the revenue obtained from customers indeed exceeds the payment to generators, thereby confirming revenue adequacy under the proposed dynamics-aware pricing of reserves.

3) Generator Cost Recovery: We evaluate each generator's ability to recover its cost by verifying that the cost satisfies

$$\sum_{t\in\mathcal{T}^{\mathrm{D}}_{t_0}} C_g(\overline{P}^{\mathrm{m}\star}_{g,t})\Delta t^{\mathrm{D}} \leq \sum_{t\in\mathcal{T}^{\mathrm{D}}_{t_0}} \Big(\frac{1}{\Delta t^{\mathrm{D}}}\frac{\partial \mathcal{L}^{\star}}{\partial \overline{P}^{\mathrm{load}}_t}\Big)\overline{P}^{\mathrm{g}\star}_{g,t}\Delta t^{\mathrm{D}} + \sum_{t\in\mathcal{T}^{\mathrm{D}}_{t_0}} \Lambda^{\star}_t \sigma^P_{g,t}\Delta t^{\mathrm{D}},\ \forall\, g\in\mathcal{G}, \tag{41}$$

where the right-hand side comprises generator g's revenue for energy production and for setting aside reserves (i.e., the components of (38) associated with generator g). Above, $\overline{P}^{\mathrm{g}\star}_{g,t}$ is the optimal average electrical power output from generator g at time t, which can be evaluated given the optimal decisions solved from (27) as

$$\overline{P}^{\mathrm{g}\star}_{g,t} = \overline{P}^{\mathrm{m}\star}_{g,t} - D_g\Delta\overline{\omega}^{\star}_t - M_g\Big(\frac{\Delta\overline{\omega}^{\star}_{t+\Delta t^{\mathrm{D}}} - \Delta\overline{\omega}^{\star}_t}{\Delta t^{\mathrm{D}}}\Big),\quad t\in\mathcal{T}^{\mathrm{D}}_{t_0}\setminus\{t_0+T\}. \tag{42}$$

In Table IV, we report revenues and costs for each generator and verify that, in all cases, each generator's revenue is indeed sufficient to recover its cost.

TABLE V: Time [sec] incurred to solve the dynamics-aware CCED for various lengths of scheduling horizons in case studies involving the WSCC and New England test systems.

Length of Scheduling Horizon [sec]	100	200	300	600
WSCC (3 generators)	1.21	3.05	6.17	13.3
New England (10 generators)	2.48	5.13	9.73	20.2

C. Computational Scalability

In Table V, we report the combined computation time incurred to compile the dynamics-aware CCED in the MATLAB YALMIP toolbox and to solve it using MOSEK for the WSCC and the New England test systems. Here, we impose random variations between -5% and $+5\%$ every $20\,[\mathrm{sec}]$ in the forecast of each load in a test system and solve the dynamics-aware CCED for various lengths of scheduling horizons ranging from 100 to $600\,[\mathrm{sec}]$. As shown in Table V, computation times grow with longer scheduling horizons but remain well within them for both test systems. All numerical results are obtained from case studies performed on a typical desktop computer with a $3.6\,[\mathrm{GHz}]$ i7 processor and $32\,[\mathrm{GB}]$ RAM.

VI. Concluding Remarks

This paper presented a method to compute dynamics-aware real-time pricing of reserves accompanying the optimal solution of a CCED constrained by system frequency dynamics arising from generators and the AGC. Given uncertainty in the net-load forecast across the scheduling horizon, chance constraints enforce tolerable probability of dynamic system frequency and generator power trajectories violating their respective limits. The dynamics-aware CCED reformulates into a deterministic optimization problem, and we derived the price of reserves from its optimal Lagrangian. Numerical simulations demonstrate the benefit of the dynamics-aware price of reserves in providing more revenue and profit for generators that tune their dynamic parameters to contribute to improved system dynamic performance characterized by metrics like risk of violating frequency constraints. While case studies demonstrate system reserve revenue adequacy and generator cost recovery numerically, a compelling direction for future work is more rigorous analysis of key market properties. Future work also includes incorporating chance constraints on line flows via injection shift factors into the CCED to study transmission-constrained dynamics-aware price of reserves.

References

[1] T. Mai, R. Wiser, G. Barbose, L. Bird, J. Heeter, D. Keyser, V. Krishnan, J. Macknick, and D. Millstein, "A prospective analysis of the costs, benefits, and impacts of us renewable portfolio standards," National Renewable Energy Laboratory, Golden, CO, Tech. Rep., Dec. 2016.

[2] K. Van den Bergh and E. Delarue, "Energy and reserve markets: interdependency in electricity systems with a high share of renewables," *Electr. Power Syst. Res.*, vol. 189, p. 106537, 2020.

[3] J. F. Ellison, L. S. Tesfatsion, V. W. Loose, and R. H. Byrne, "Project report: a survey of operating reserve markets in us iso/rto-managed electric energy regions." Sandia National Laboratories, Albuquerque, NM, Tech. Rep., 2012.

[4] D. S. Kirschen and G. Strbac, *Fundamentals of power system economics*. John Wiley & Sons, 2018.

[5] "Co-optimization information document," Alberta Electric System Operator, 2024.

[6] "PJM manual 11: Energy & ancillary services market operations, revision 134," PJM, 2025.

[7] P. González, J. Villar, C. A. Díaz, and F. A. Campos, "Joint energy and reserve markets: Current implementations and modeling trends," *Electr. Power Syst. Res.*, vol. 109, pp. 101–111, 2014.

[8] J. Chen, T. D. Mount, J. S. Thorp, and R. J. Thomas, "Location-based scheduling and pricing for energy and reserves: a responsive reserve market proposal," *Decision Support Syst.*, vol. 40, pp. 563–577, 2005.

[9] S. Just and C. Weber, "Pricing of reserves: Valuing system reserve capacity against spot prices in electricity markets," *Energy Econ.*, vol. 30, no. 6, pp. 3198–3221, Nov. 2008.

[10] A. Papavasiliou, S. S. Oren, and R. P. O'Neill, "Reserve requirements for wind power integration: A scenario-based stochastic programming framework," *IEEE Trans. Power Syst.*, vol. 26, no. 4, pp. 2197–2206, Nov. 2011.

[11] H. Ye, Y. Ge, M. Shahidehpour, and Z. Li, "Uncertainty marginal price, transmission reserve, and day-ahead market clearing with robust unit commitment," *IEEE Trans. Power Syst.*, vol. 32, no. 3, pp. 1782–1795, May 2017.

[12] Y. Dvorkin, "A chance-constrained stochastic electricity market," *IEEE Trans. Power Syst.*, vol. 35, no. 4, pp. 2993–3003, Jul. 2020.

[13] G. Zhang, J. McCalley, and Q. Wang, "An AGC dynamics-constrained economic dispatch model," *IEEE Trans. Power Syst.*, vol. 34, no. 5, pp. 3931–3940, Apr. 2019.

[14] R. Khatami, M. Parvania, C. Chen, S. S. Guggilam, and S. V. Dhople, "Dynamics-aware continuous-time economic dispatch: A solution for optimal frequency regulation." in *Proc. Hawaii Int. Conf. Syst. Sci.*, Jan. 2020, pp. 3186–3195.

[15] S. Chapaloglou, E. F. Alves, V. Trovato, and E. Tedeschi, "Optimal energy management in autonomous power systems with probabilistic security constraints and adaptive frequency control," *IEEE Trans. on Power Syst.*, vol. 39, no. 1, pp. 1543–1554, Jan. 2024.

[16] Z. Liang, R. Mieth, and Y. Dvorkin, "Inertia pricing in stochastic electricity markets," *IEEE Trans. Power Syst.*, vol. 38, no. 3, pp. 2071–2084, May 2023.

[17] L. Badesa, C. Matamala, Y. Zhou, and G. Strbac, "Assigning shadow prices to synthetic inertia and frequency response reserves from renewable energy sources," *IEEE Trans. Sustain. Energy*, vol. 14, no. 1, pp. 12–26, Jan. 2023.

[18] L. Badesa, F. Teng, and G. Strbac, "Pricing inertia and frequency response with diverse dynamics in a mixed-integer second-order cone programming formulation," *Appl. Energy*, vol. 260, p. 114334, 2020.

[19] M. Garcia, R. Baldick, and F. Wilches Bernal, "Pricing frequency response market products for inverter-based resources." Sandia National Laboratory, Albuquerque, NM (United States), Tech. Rep., 2020.

[20] K. Li, H. Guo, X. Fang, S. Liu, F. Teng, and Q. Chen, "Market mechanism design of inertia and primary frequency response with consideration of energy market," *IEEE Trans. Power Syst.*, vol. 38, no. 6, pp. 5701–5713, Nov. 2023.

[21] R. Khatami, A. Al-Digs, and Y. C. Chen, "Frequency dynamics-aware real-time marginal pricing of electricity," *Electr. Power Syst. Res.*, vol. 212, p. 108429, 2022.

[22] B. Chen, R. Khatami, A. Al-Digs, and Y. C. Chen, "Incorporating system frequency dynamics into real-time locational marginal pricing of electricity," *IEEE Trans. Power Syst.*, vol. 39, no. 2, pp. 4638–4649, Mar. 2024.

[23] B. Chen, R. Khatami, and Y. C. Chen, "Frequency dynamics-aware real-time marginal pricing of electricity under uncertainty," in *Proc. IEEE Power Energy Soc. Innov. Smart Grid Technol. Conf.*, 2024, pp. 1–5.

[24] A. J. Wood, B. F. Wollenberg, and G. B. Sheblé, *Power generation, operation, and control, 3rd Edition*. John Wiley & Sons, 2013.

[25] W. B. Gish, "Automatic generation control - notes and observations," Electric Power Branch, Division of Research, Engineering and Research Center, Tech. Rep. REC-ERC-78-6, Oct. 1978.

[26] P. Kundur, *Power system stability*. CRC Press New York, NY, USA, 2007.

[27] S. V. Dhople, Y. C. Chen, A. Al-Digs, and A. D. Domínguez-García, "Reexamining the distributed slack bus," *IEEE Trans. Power Syst.*, vol. 35, no. 6, pp. 4870–4879, Nov. 2020.

[28] M. D. Ilić and Q. Liu, *Toward Sensing, Communications and Control Architectures for Frequency Regulation in Systems with Highly Variable Resources*. New York, NY: Springer-Verlag, 2012, pp. 3–33.

[29] S. Dong and Y. C. Chen, "Adjusting synchronverter dynamic response speed via damping correction loop," *IEEE Trans. Energy Convers.*, vol. 32, no. 2, pp. 608–619, Dec. 2017.

[30] A. R. Al-Roomi, "Power Flow Test Systems Repository," Halifax, Nova Scotia, Canada, 2015. [Online]. Available: https://al-roomi.org/power-flow

[31] H. Akhavan-Hejazi and H. Mohsenian-Rad, "Energy storage planning in active distribution grids: A chance-constrained optimization with non-parametric probability functions," *IEEE Trans. Smart Grid*, vol. 9, no. 3, pp. 1972–1985, May 2018.

[32] Z. Wang, C. Shen, F. Liu, X. Wu, C.-C. Liu, and F. Gao, "Chance-constrained economic dispatch with non-gaussian correlated wind power uncertainty," *IEEE Trans. Power Syst.*, vol. 32, no. 6, pp. 4880–4893, Nov. 2017.

[33] W. Xie and S. Ahmed, "Distributionally robust chance constrained optimal power flow with renewables: A conic reformulation," *IEEE Trans. Power Syst.*, vol. 33, no. 2, pp. 1860–1867, Mar. 2018.

[34] E. Dall'Anese, K. Baker, and T. Summers, "Chance-constrained ac optimal power flow for distribution systems with renewables," *IEEE Trans. Power Syst.*, vol. 32, no. 5, pp. 3427–3438, 2017.

[35] L. Roald and G. Andersson, "Chance-constrained ac optimal power flow: Reformulations and efficient algorithms," *IEEE Trans. Power Syst.*, vol. 33, no. 3, pp. 2906–2918, 2017.

[36] Y. Song, T. Liu, and D. J. Hill, "Chance constrained economic dispatch considering the capability of network flexibility against renewable uncertainties," *IEEE Trans. Power Syst.*, 2024.

[37] S. Xu and W. Wu, "Tractable reformulation of two-side chance-constrained economic dispatch," *IEEE Trans. Power Syst.*, vol. 37, no. 1, pp. 796–799, 2022.

[38] W. Xie, S. Ahmed, and R. Jiang, "Optimized Bonferroni approximations of distributionally robust joint chance constraints," *Math. Program.*, vol. 191, no. 1, pp. 79–112, 2022.

[39] A. M. Fathabad, J. Cheng, K. Pan, and B. Yang, "Asymptotically tight conic approximations for chance-constrained ac optimal power flow," *Eur. J. of Oper. Res.*, vol. 305, no. 2, pp. 738–753, 2023.

[40] Illinois Center for a Smarter Electric Grid (ICSEG), "IEEE 39-Bus System (10-Machine New England Power System)," 2025. [Online]. Available: https://icseg.iti.illinois.edu/ieee-39-bus-system/

[41] F. Milano, "An open source power system analysis toolbox," *IEEE Trans. Power Syst.*, vol. 20, no. 3, pp. 1199–1206, Aug. 2005.